Nature Environment and Pollution Technology *An International Quarterly Scientific Journal*	p-ISSN: 0972-6268 e-ISSN: 2395-3454	Vol. 16	No. 4	pp. 1035-1042	2017

Original Research Paper **Open Access**

Analysis of the Relationship Between Land Surface Temperature and Land Cover Changes Using Multi-temporal Satellite Data

Qingkong Cai*(**)†, Erjun Li* and Ruibo Jiang***

*College of Civil Engineering, Henan University of Engineering, Zhengzhou 451191, China

**Henan Province Engineering Laboratory of Comprehensive Utilization of Coal Resources and Pollution Control, Zhengzhou 451191, China

***College of Human and Social Sciences, Henan University of Engineering, Zhengzhou 451191, China

†Corresponding author: Qingkong Cai

Nat. Env. & Poll. Tech.
Website: www.neptjournal.com

Received: 15-06-2017
Accepted: 18-08-2017

Key Words:
Land surface temperature
Land cover change
Zhengzhou
Remote sensing

ABSTRACT

Rapid urbanization, coupled with the tremendous growth in population and built-up areas in cities, leads to problems associated with global climate change impacts, such as urban heat island effect, which influences regional climate, urban environmental pollution, and socio-economic development. This study aims to detect the spatial variation of land surface temperature (LST) and determine its quantitative relationship with land cover types using the techniques of remote sensing and geographic information system. Taking the city of Zhengzhou as the study area, we utilized four Landsat TM images from 1988 to 2017 to classify land cover types by maximum likelihood classification and retrieve the LST by using a mono-window algorithm. Results show that the urban heat island areas have an expanding trend from 1988 to 2017 in general. Moreover, the spatial distribution pattern and extension of the urban heat islands are consistent with urban sprawl. Changes in land cover type altered the spatial distribution characteristics of LST from 1988 to 2017. In various land cover types, the construction land and bare land showed the highest temperature, and they significantly contributed to the heat island effect. Green land and water can effectively relieve the heat island effect. Finally, constructive strategies and measures to alleviate the urban heat island effect are proposed from different aspects. Therefore, this work provides a scientific reference for decision making to improve the thermal environment and achieve sustainable development in the future.

INTRODUCTION

The rapid urbanization process brings about economic prosperity and civilization progress. However, it also causes a series of ecological and environmental problems, one of which is the urban heat island effect. Under the urban heat island effect, the urban temperature is higher than the temperature in the surrounding suburbs (Howard 1833). The heat island effect increases the city temperature and worsens the urban climate comfort. The heat island circulation increases the pollution of the urban environment and adversely affects the improvement of urban air quality, haze governance, and plant health growth. The rapid development of a city changes the land types and the nature of the underlying surface. The original water-permeable surface covered by plants is replaced by impervious surfaces, such as roads, buildings, and others. Studies have shown that changes in land cover type and human production and lifestyle mainly drive the generation and evolution of the urban heat island effect (Lei et al. 2016). Therefore, research into the causes, spatial distribution, and dynamic changes of the urban heat island effect and the impact of land cover change on the land surface temperature (LST), would help to solve urban environmental problems. Such study would also provide the necessary technical support and theoretical basis for building a livable, green, and safe residential environment and ensuring sustainable development.

In recent decades, the study of the urban heat island effect has made great progress in terms of the research area, scale, content, depth, and methods (Hausfather et al. 2013, Benali et al. 2012, Dou et al. 2011, Li et al. 2013). Xia et al. took Xuzhou City as an example and carried out quantitative studies on the spatial distribution characteristics of heat islands and the relationship between LST and land cover type (Xia et al. 2010). Duan et al. analysed the land cover change and heat island effect of Zhengzhou and found that the acceleration of urbanization is the main reason behind the land cover change and that the heat island effect of Zhengzhou is continuously increasing (Duan et al. 2011, Duan et al. 2013). Zhang et al. performed a systematic study on the temporal and spatial distribution characteristics of the land cover and heat island effect of Fuzhou and its surrounding areas using remote sensing images of two differ-

Table 1: Area statistics of LST levels of Zhengzhou in 1988, 1999, 2011 and 2017 (unit: km^2).

Grades	1988		1999		2011		2017	
	Area	Percentage	Area	Percentage	Area	Percentage	Area	Percentage
Low LST	188.73	17.83%	192.58	18.19%	172.11	16.26%	99.54	9.41%
Sub-middle LST	186.55	17.62%	181.53	17.15%	126.65	11.96%	114.53	10.82%
Middle LST	352.25	33.28%	325.15	30.72%	375.55	35.48%	527.75	49.88%
Sub-high LST	137.71	13.01%	146.86	13.87%	217.29	20.53%	227.64	21.51%
High LST	193.28	18.26%	212.40	20.07%	166.92	15.77%	88.67	8.38%

Table 2: Area statistics of land use types from 1988 to 2017.

Land use type	Area/km^2				Total change/km^2	Annual change rate(%)		
	1988	1999	2011	2017	1988-2017	1988-1999	1999-2011	2011-2017
Construction land	244.24	327.31	586.20	653.17	408.93	3.09	6.59	1.90
Green land	466.26	503.65	352.21	342.42	-123.84	0.73	-2.51	-0.46
Water	110.63	81.32	64.24	41.60	-69.03	-2.41	-1.75	-5.87
Bare land	237.39	146.24	55.87	21.332	-216.06	-3.49	-5.15	-10.30

Table 3: LST characteristics of different land cover types.

Land use type	1988		1999		2011		2017	
	average LST	std	average LST	std	average LST	std	average LST	std
Construction land	27.76	2.64	34.07	2.81	32.36	2.55	30.47	2.29
Green land	23.84	2.50	29.73	2.78	27.44	2.59	28.38	3.03
Water	20.47	3.73	26.81	2.47	22.64	4.11	18.49	6.30
Bare land	30.64	2.95	36.94	2.44	32.48	2.26	24.12	7.40

ent phases (Zhang et al., 2011). Jia et al. retrieved the surface temperature of Xining using geographic information system (GIS) spatial analysis techniques and single window algorithms and later revealed that the spatial distribution pattern and extension of the urban heat island is consistent with urban sprawl and that the heat island effect is the strongest in winter, followed by summer and autumn (Jia et al. 2014). Jiang et al. analysed the influence of land cover changes on LST for the period of over 20 years in Beijing and concluded that the spatial distribution of LST is obviously consistent with the spatial pattern of land cover types (Jiang et al. 2014). Qian et al. studied the land cover changes in the Pearl River Delta region, especially the effects of urban growth on surface temperature (Qian et al. 2005). On the basis of the Landsat TM/ETM+ data in 1993, 2001, and 2011, Pan retrieved the LST of Lanzhou and conducted thermal field division, followed by an analysis of the temporal and spatial characteristics of the urban heat island in Lanzhou (Pan 2016). On the basis of MODIS and TM data, Tran et al. analysed the thermal states of the cities of Tokyo, Beijing, Shanghai, Seoul, Pyongyang, Bangkok, Manila, and Ho Chi Minh; and then studied the relationship between the diurnal and seasonal variation characteristics and vegetation status, the spatial distribution patterns of thermal fields, and city thermal radiation (Tran et al. 2006). Pandey et al. studied the heat islands of Delhi using MODIS-based ground temperature data and found that nocturnal heat islands exist throughout the year and that heat island intensity is negatively correlated with aerosol optical thickness (Pandey et al. 2014). Weng et al. conducted a spatio-temporal comparative analysis on the effects of land cover changes on the urban thermal field in Guangzhou (Weng et al. 2004). The research of Jr Stone indicated that the mean decadal change rate of heat island intensity reached 0.05°C between 1951 and 2000 in large US cities; the result also revealed a difference in heat island intensity in the northeastern and southern regions of the country (Jr Stone 2007). Weng et al. employed mixed pixel decomposition to obtain information about water-impermeable surfaces and vegetation coverage and then explained the urbanization process of Indiana on the basis of the changes in coverage and surface temperature (Weng et al. 2008). In

general, holistic and systematic research on the effects of land cover types on LST remains lacking.

Currently, many studies on the temporal and spatial evolution of the heat island effect have been carried out, and the study area is mostly concentrated in first-tier cities, such as Beijing and Shanghai. At the same time, the influence mechanism of different land cover types on LST has yet to be systematically studied, and little attention has been paid to the rapidly developing central areas of China. On the basis of the above analysis, this study takes the city of Zhengzhou as the study area and uses four TM images from 1988, 1999, 2011, and 2017 as the data sources. We analyzed the impact of land cover changes on the heat island effect, so as to provide scientific reference and decision support for improving the urban human settlement and weakening the urban heat island effect for Zhengzhou.

MATERIALS AND METHODS

Study area: Zhengzhou is located in the south of Huabei Plain, which lies in the northern region of central Henan in China (112°42'E to 114°13'E, 34°16 'N to 34°58'N). It has a width of 166 km from east to west and 75 km from north to south. The terrain is gradually inclined from southwest to northeast, and the elevation ranges from 73 m to 1512.4 m, with an average elevation of 110 m. The area belongs to a typical temperate continental monsoon climate, the average annual temperature is 14.4°C, the average annual rainfall is 640.9 mm, and the frost-free period is 220 days. The area has six districts (Zhongyuan, Erqi, Jinshui, Huiji, Guancheng, and Shangjie), five county-level cities (Gongyi, Xinzheng, Dengfeng, Xinmi, and Xingyang), and one county (Zhongmou). The six districts of Zhengzhou are selected as the study area (red area in Fig. 1).

Data acquisition and pretreatment: In the study, four TM images (May 14, 1988; May 13, 1999; May 14, 2011; and April 28, 2017) of Zhengzhou were selected as the data source. The images shared the same acquisition time and high quality. First, the radiometric calibration and atmospheric correction of three of the four images were carried out. The images from 1988, 1999, and 2011 were then registered on the basis of the image from 2017. The registration error was controlled within 0.5 pixels. Finally, we used the vector data of Zhengzhou area to cut the four images and finally obtained four images of the study area.

Land surface temperature inversion: The LST was retrieved by using the single window algorithm proposed by Qin Zhihao (Qin et al. 2001). The specific steps of the inversion are as follows:

The first step was to convert the pixel *DN* value to the radiation luminance value *L*.

$$L = L_{\min} + (L_{\max} - L_{\min})DN/255 \quad ...(1)$$

Where, $L_{\max} = 1.56 mW/(cm^2 \cdot sr)$,

$L_{\min} = 0.1238 mW/(cm^2 \cdot sr)$ for the Landsat TM image.

The second step was to convert the radiation luminance value L to the brightness temperature value T_6.

$$T = K_2/\ln(1 + K_1/L) \quad ...(2)$$

Where, T is the brightness temperature, L is the radiation luminance value, K_1 and K_2 are the pre-set constants before launch, i.e., $K_1 = 60.776 mW/(cm^2 \cdot sr \cdot \mu m)$, $K_2 = 1260.56K$.

The third step was to retrieve the true LST T_S.

$$T_S = \{a(1-C-D) + [b(1-C-D) + C + D]T - DT_a\}/C \quad ...(3)$$

Where, $C = \tau\varepsilon$, $D = (1-\tau)[1+\tau(1-\varepsilon)]$, $a = -60.3263$, $b = 0.43436$, and T_a is the average atmospheric temperature, which is estimated approximately by using the near surface atmospheric temperature T_0. T_0 can be obtained using meteorological weather information.

$$T_a = 16.0110 + 0.92621T_0 \quad ...(4)$$

where τ is the atmospheric transmittance, which is estimated through the following empirical formula (Qin et al. 2001):

$$\tau = 1.031412 - 0.11536w \quad ...(5)$$

Where w is the atmospheric precipitation (g/cm^2) of the whole layer that can be calculated through the formula $w = 0.1965 + 0.1755e$; e is the actual water vapour pressure (*hPa*) of the ground (Yang et al. 2002).

Variable ε is the surface emissivity estimated by the method proposed by Qin Zhihao and Jose (Qin et al. 2001, 2003, Jose et al. 2004). When, $NDVI < 0.05$, take $\varepsilon = 0.973$.

When, $NDVI > 0.70$ take $\varepsilon = 0.99$.

When, $0.05 \le NDVI \le 0.70$, the formula is

$$\varepsilon = 0.004P_V + 0.986 \quad ...(6)$$

Where $P_V = [(NDVI - NDVI_{soil})/(NDVI_{veg} - NDVI_{soil})]^2$, P_v is the vegetation coverage, and $NDVI_{veg}$ and $NDVI$ are the values of bare soil and vegetation, respectively. Given the lack of spectral data of bare soil and vegetation, we adopted the experience value ($NDVI_{soil} = 0.05$, $NDVI_{veg} = 0.70$) to estimate the vegetation coverage. Thereafter, the LST values of Zhengzhou in 1988, 1999, 2011, and 2017 were obtained via emissivity correction using the surface emissivity data (Fig. 2).

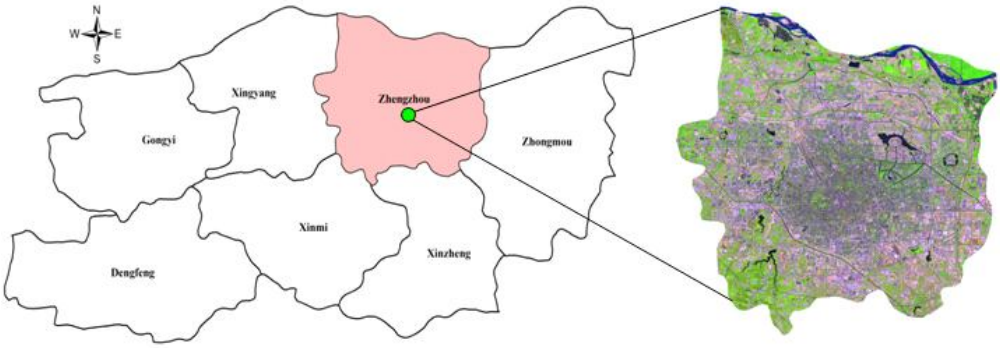

Fig. 1: Geographical location map of the study area.

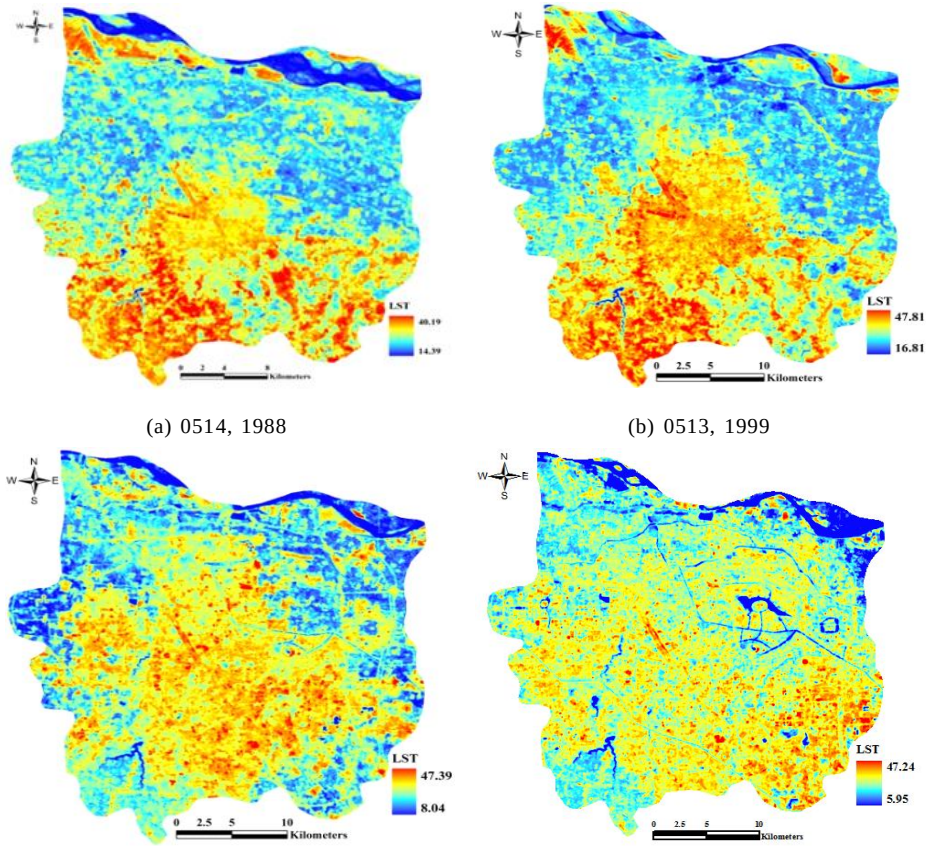

(a) 0514, 1988 (b) 0513, 1999

(c) 0514, 2011 (d) 0428, 2017

Fig. 2: Land surface temperature distribution of Zhengzhou city.

Land cover classification: The land use types of Zhengzhou were divided into the following four types according to the types of urban land use and its functional characteristics: construction land, green land, water, and bare land. On the basis of the characteristics of image hue and texture, the sample and verification points of the four land use types were selected in the homogeneous region of the three remote sensing images according to the ratio of 6:4. Then, we used the maximum likelihood method to classify the four remote sensing images. The classification results were then edited and processed to obtain the four land cover classification maps of Zhengzhou (Fig. 3). The classification re-

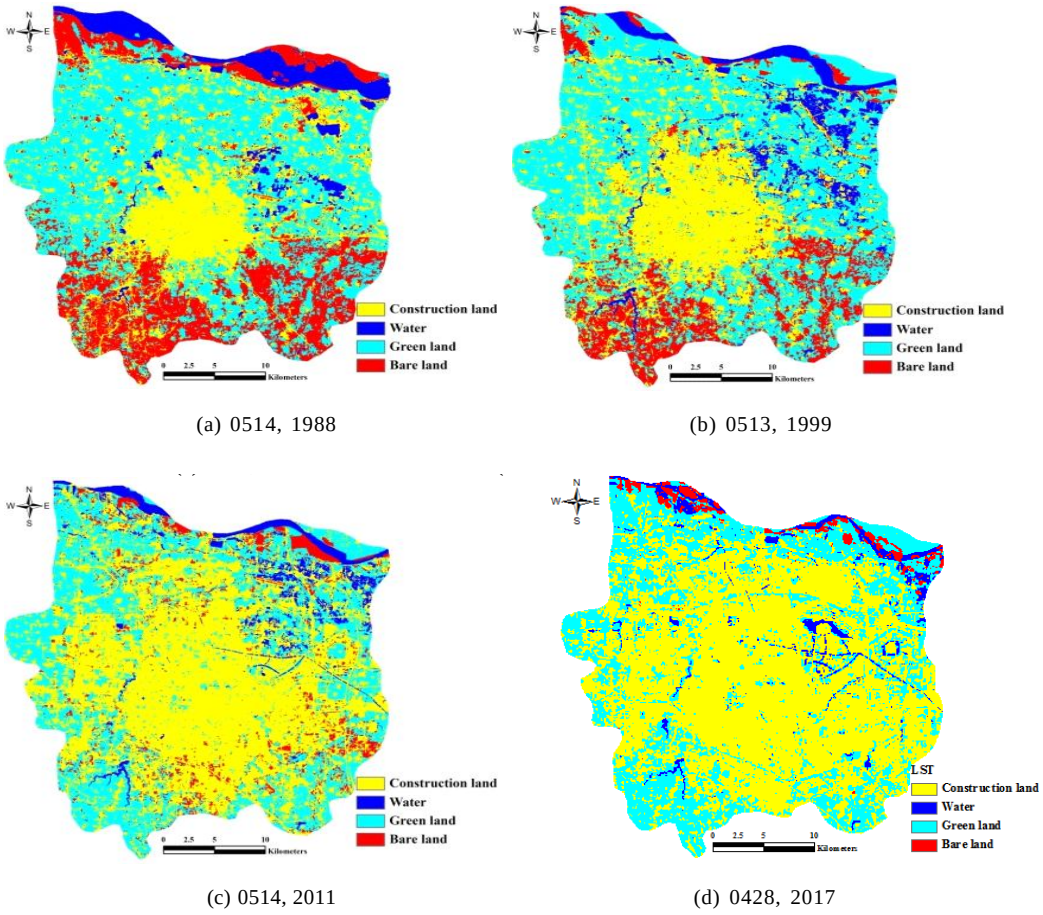

(a) 0514, 1988 (b) 0513, 1999

(c) 0514, 2011 (d) 0428, 2017

Fig. 3: Land cover classification maps of Zhengzhou city.

sults were verified to meet the research requirements.

RESULTS AND DISCUSSION

Temporal and spatial evolution of land surface temperature: Currently, heat island classification is performed using two methods: equal spacing and mean-standard deviation method. The mean-standard deviation method usually combines the mean temperature (μ) and standard deviation (*std*) to divide the temperature grade; it can effectively overcome the subjectivity of temperature stratification number and segmentation threshold (Zhang et al. 2005, Chen et al. 2009). Therefore, we used this method to divide the LST image into five levels: high temperature region ($LST > \mu + std$), sub-high temperature region ($\mu + 0.5std < LST \le \mu + std$), middle temperature region ($\mu - 0.5std < LST \le \mu + 0.5std$), sub-middle temperature region ($\mu - std < LST \le \mu - 0.5std$), and low temperature region ($LST \le \mu - std$); in this study, μ is the mean value, and *std* is the standard deviation. According to the division standard, we obtained the surface temperature level map of Zhengzhou (Fig. 4).

Through statistics, we obtained the area of five surface temperature gradients of the four images of Zhengzhou (Table 1).

From 1988 to 1999, the area of the middle temperature zone decreased while those of the high temperature and sub-high temperature zones increased. The area of the high temperature zone increased to 19.12 km^2. From 1999 to 2011, the areas of the middle temperature and sub-high temperature zones increased, with their proportions increasing from 30.72% and 13.87% in 1999 to 35.48% and 20.53% in 2011, respectively. Moreover, the areas of the low temperature, sub-middle temperature, and high temperature zones decreased. The area of the high temperature zone decreased to 45.48 km^2. From 2011 to 2017, the areas of the middle temperature and sub-high temperature zones increased, with

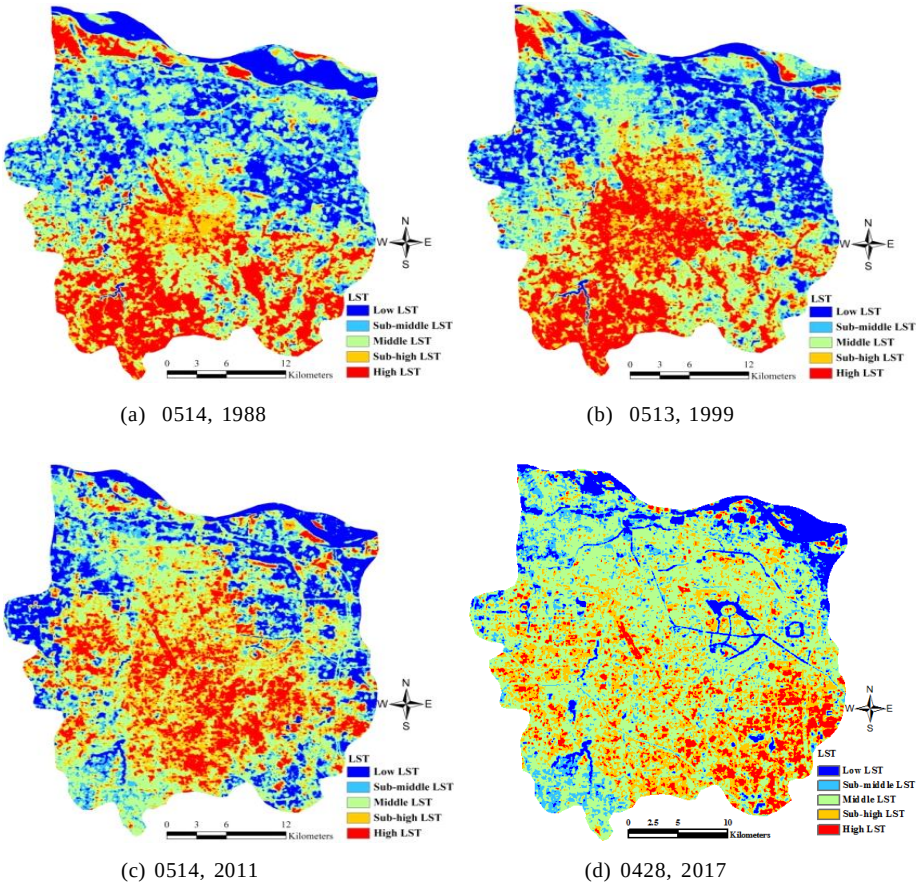

(a) 0514, 1988 (b) 0513, 1999

(c) 0514, 2011 (d) 0428, 2017

Fig. 4: Grade of land surface temperature of Zhengzhou city.

their proportions increasing from 35.48% and 20.53% in 2011 to 49.88% and 21.51% in 2017, respectively. Moreover, the areas of the low temperature, sub-middle temperature, and high temperature zones decreased. The area of the high temperature zone decreased to 78.25 km^2. This phenomenon is closely related to the development of urbanization and the changes in land cover. Referring to Fig. 4, we concluded that the area of the high temperature zone in the southwest of Zhengzhou decreased with the increase of vegetation coverage (1999-2011).

Overall characteristics of land cover change: The land cover change matrix of the study area was extracted through a land cover classification map, as shown in Table 2. The table shows that the land use pattern of Zhengzhou changed greatly from 1988 to 2017. The construction land increased by 167%, especially in the period of 1999-2011. The construction land increased rapidly, with the annual average rate of change reaching 6.59%. These findings confirmed the rapid urbanization process of Zhengzhou. The areas of green land, water, and bare land decreased from 1988 to 2017, and the amplitude of bare land was the largest, reaching 91.01%, followed by those of green land and water, whose areas of reduction were 123.84 and 69.03 km^2, respectively.

Influences of land cover changes on land surface temperature: To analyse the effects of different land cover types on LST, we calculated the average surface temperature and standard deviation of different land cover types and the number of land cover types in different temperature ranges. The results are shown in Table 3 and Fig. 5.

In the different types of land cover, the temperatures of bare land and construction land were the highest, followed by those of green land and water. The construction land and bare land were superior in the high and sub-high temperature regions. Water and green land accounted for a large proportion in the low and middle temperature regions. The results indicate that the construction land and bare land were the main factors that contributed to urban heat island intensity. Water and green land exerted a cooling effect on the surface temperature. Such effect, in turn, was critical to

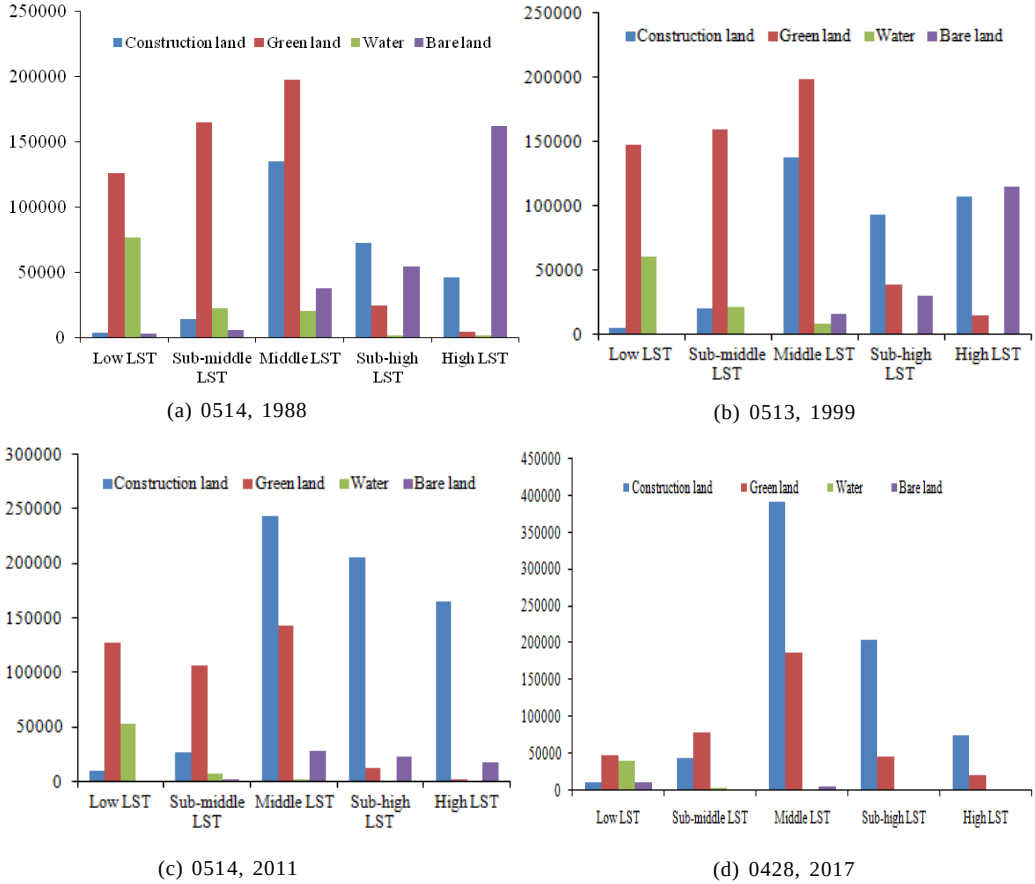

Fig. 5: Land cover change proportions of LST grades in 1988, 1999, 2011 and 2017.

segmenting and controlling the urban heat island distribution. From 1988 to 1999, the temperatures of the four land cover types, i.e., construction land, green land, water, and bare land, all increased from 27.76°C, 23.84°C, 20.47°C, and 30.64°C, respectively, to 34.07°C, 29.73°C, 26.81°C, and 36.94°C, respectively. From 1999 to 2011, the temperatures of all types decreased from 34.07°C, 29.73°C, 26.81°C, respectively and 36.94°C to 32.36°C, 27.44°C, 22.64°C, and 32.48°C respectively. From 2011 to 2017, the temperatures of three land cover types, i.e., construction land, water, and bare land, all decreased from 32.36°C, 22.64°C, and 32.48°C, respectively, to 30.47°C, 18.49°C, and 24.12°C, respectively. The average temperature of each land use type increased from 1999 to 2011. In comparison with the heat island intensity in 1999, the heat island intensity in recent years (2011, 2017) was alleviated to a certain extent. At the same time, the range of heat island effect increased year by year, thereby indicating that Zhengzhou made some achievements in urban greening and water construction. Nevertheless, the heat island effect of Zhengzhou showed an increasing trend (1988-2017).

CONCLUSIONS

High urban temperature should be alleviated, and the development of cities should rationally be planned. In this study, four Landsat TM images of Zhengzhou were utilized to classify land cover types via maximum likelihood classification and to retrieve the LST by using a mono-window algorithm. A quantitative analysis was conducted between land cover changes and LSTs in the past 30 years on the basis of GIS technology. The following conclusions could be drawn.

1. The acceleration of urbanization leads to significant changes in land use types, especially construction land. With the rapid development of cities, the range of heat island effect is expanding, and the intensity obviously increases. The distribution and extension of thermal field are consistent with urban expansion.
2. The surface temperatures of different land cover types differ. Construction land and bare land have the highest temperature and are thus the main factors that contribute to the urban heat island effect. The temperatures of

green land and water are relatively low. Thus, increasing the areas of urban green land and water plays an important role in alleviating the urban heat island effect.

3. The changes in land cover type alter the spatial distribution of surface temperature. The main reason lies in the natural change of the underlying surface caused by changes in land cover type. The changes in the underlying surface result in changes in the LST. Therefore, the changes in the land cover type are important drivers of urban surface temperature.

This study quantitatively analyzed the impact of land cover changes on LST and proposed measures and countermeasures for alleviating the urban heat island effect. However, the influences of environmental factors (elevation, slope, aspect, and vegetation coverage) on the urban heat island effect were not deeply discussed and should thus be considered in future studies.

ACKNOWLEDGEMENTS

This work was supported by Open Fund Program of Henan Engineering Laboratory of Pollution Control and Coal Chemical Resources Comprehensive Utilization (502002-02) and Doctoral Fund of Henan Institute of Engineering (D2016005).

REFERENCES

Benali, A., Carvalho, A.C. and Nunes, J.P. et al. 2012. Estimating air surface temperature in Portugal using MODIS LST data. Remote Sensing of Environment, 124(9): 108-121

Chen, S.L. and Wang, T.X. 2009. Comparison analyses of equal interval method and mean-standard deviation method used to delimitate urban heat island. Journal of Geo-Information Science, 11(2): 145-150.

Dou, H. and Zhao, X. 2011. Climate change and its human dimensions based on GIS and meteorological statistics in Pearl River Delta, Southern China. Meteorological Applications, 18(1): 111-122

Duan, J.L., Song, X. and Zhang, X.L. 2011. Temporal and spatial evolution of urban heat island effect in Zhengzhou based on RS. Chinese Journal of Applied Ecology, 22(1): 165-170.

Duan, J.L., Zhang, X.L. and Wang, Y.L. 2013. Remote sensing monitoring and analysis of land resources transformation in Zhengzhou. Journal of Henan University of Science and Technology: Natural Science, 34(1): 98-100.

Hausfather, Z., Menne, M.J. and Williams, C.N. et al. 2013. Quantifying the effect of urbanization on US historical climatology network temperature records. Journal of Geophysical Research: Atmospheres, 118(2): 481-494.

Howard, L. 1833. Climate of London Deduced from Metrological Observations. London: Harvey and Dolton Press.

Jiang, J.B., Cai, Q.K. and Cui, X.M. et al. 2014. Influence of land cover change on land surface temperature in Beijing. Journal of Henan University of Science and Technology: Natural Science, 35(3): 100-104.

Jia, W. and Gao, X.H. 2014. Analysis of urban heat island environment in a valley city for policy formulation: a case study of Xining city in Qinghai province of China. Journal of Geo-information Science, 16(4): 592-601.

Sobrino, J.A., Jimenez-Munoz, J.C. and Paolini, L. 2004. Land surface temperature retrieval from Landsat TM5. Remote Sensing of Environment, 90(4): 434-440.

Jr Stone, B. 2007. Urban and rural temperature trends in proximity to large US cities: 1951-2000. International Journal of Climatology, 27(13): 1801-1807.

Lei, C.M., Zhou, Q. and Zhang, C. et al. 2016. Temporal and spatial evolution of surface temperature inversion and urban heat island distribution pattern in Baoji City. Journal of Baoji University of Arts and Sciences (Nature Science), 36(3): 45-51.

Li, Y., Zhu, L. and Zhao, X. et al. 2013. Urbanization impact on temperature change in China with emphasis on land cover change and human activity. Journal of Climate, 26(22): 8765-8780.

Pandey, A.K., Singh, S. and Berwal, S. et al. 2014. Spatiotemporal variations of urban heat island over Delhi. Urban Climate, 10: 119-133.

Pan, J.H. 2016. Area delineation and spatial-temporal dynamics of urban heat island in Lanzhou city, China using remote sensing imagery. Journal of the Indian Society of Remote Sensing, 44(1): 111-127.

Qian, L.X. and Ding, S.Y. 2005. Influence of land cover change on land surface temperature in Zhujiang Delta. Acta Geographica Sinica, 60(5): 761-770.

Qin, Z.H., Karnieli, A. and Berliner, P. 2001. A mono-window algorithm for retrieving land surface temperature from Landsat TM data and its application to the Israel-Egypt border region. International Journal of Remote Sensing, 22(18): 3719-3746.

Qin, Z.H., Li, W.J. and Zhang, M.H. et al. 2003. Estimating of the essential atmospheric parameters of mono-window algorithm for land surface temperature retrieval from landsat TM6. Remote Sensing for Land & Resources, 15(2): 37-43.

Tran, H., Daisuke, U. and Shiro, O. et al. 2006. Assessment with satellite data of the urban heat island effects in Asian megacities. International Journal of Applied Earth Observation and Geoinformation, 8: 34-48.

Weng, Q. and Yang, S.H. 2004. Managing the adverse thermal effects of urban development in a densely populated Chinese city. Journal of Environmental Management, 70(2): 145-146.

Weng, Q.H. and Lu, D.S. 2008. A sub-pixel analysis of urbanization effect on land surface temperature and its interplay with impervious surface and vegetation coverage in Indianapolis, United States. International Journal of Applied Earth Observation, 10(1): 68-83.

Xia, J.S., Du, P.J. and Zhang, H.R. et al. 2010. The quantitative relationship between land surface temperature and land cover types based on remotely sensed data. Remote Sensing and Technology and Application, 25(1): 15-23.

Yang, J.M. and Qiu, J.H. 2002. A method for estimating perceptible water and effective water vapor content from ground humidity parameters. Chinese Journal of Atmospheric Sciences, 26(1): 9-22.

Zhang, Y.S., Han, C.F. and Wu, X.C. et al. 2011. Analysis of land cover and urban thermal characteristics for Fuzhou using multi-temporal satellite data. Resources Science, 33(5): 950-957.

Zhang, Z.M., He, G.J. and Xiao, R.B. et al. 2005. A study of the urban heat island changes of Beijing city based on remote sensing. Remote Sensing Information, (6): 46-48.